Title

Conditional Loss of Arx From the Developing Dorsal Telencephalon Results in Behavioral Phenotypes Resembling Mild Human ARX Mutations

Journal

Cerebral Cortex, 25(9)

ISSN

1047-3211

Authors

Simonet, Jacqueline C
Sunnen, C Nicole
Wu, Jue
et al.

Publication Date

2015-09-01

DOI

10.1093/cercor/bhu090

Peer reviewed

Cerebral Cortex September 2015;25:2939–2950
doi:10.1093/cercor/bhu090
Advance Access publication May 2, 2014

Conditional Loss of Arx From the Developing Dorsal Telencephalon Results in Behavioral Phenotypes Resembling Mild Human *ARX* Mutations

Jacqueline C. Simonet[1], C. Nicole Sunnen[4], Jue Wu[2], Jeffrey A. Golden[4], and Eric D. Marsh[3,5]

[1]Cell and Molecular Biology Graduate Group, [2]Department of Radiology, [3]Division of Child Neurology, Children's Hospital of Philadelphia, Department of Neurology and Pediatrics, Perelman School of Medicine at the University of Pennsylvania, Philadelphia, PA, USA, [4]Department of Pathology, Children's Hospital of Philadelphia, Philadelphia, PA, USA and [5]Current address: Division of Child Neurology, Children's Hospital of Philadelphia, 3615 Civic Center Boulevard, Philadelphia, PA 19072, USA

Jeffrey A. Golden and Eric D. Marsh contributed equally to this work. Jeffrey A. Golden is now in the Department of Pathology, Brigham and Women's Hospital, Boston, Massachusetts.

Address correspondence to Eric D. Marsh, Division of Child Neurology, Children's Hospital of Philadelphia, 3615 Civic Center Boulevard, Philadelphia, PA 19072, USA. Email: marshe@email.chop.edu

Mutations in the *Aristaless-Related Homeobox* (*ARX*) gene cause structural anomalies of the brain, epilepsy, and neurocognitive deficits in children. During forebrain development, *Arx* is expressed in both pallial and subpallial progenitor cells. We previously demonstrated that elimination of *Arx* from subpallial-derived cortical interneurons generates an epilepsy phenotype with features overlapping those seen in patients with *ARX* mutations. In this report, we have selectively removed *Arx* from pallial progenitor cells that give rise to the cerebral cortical projection neurons. While no discernable seizure activity was recorded, these mice exhibited a peculiar constellation of behaviors. They are less anxious, less social, and more active when compared with their wild-type littermates. The overall cortical thickness was reduced, and the corpus callosum and anterior commissure were hypoplastic, consistent with a perturbation in cortical connectivity. Taken together, these data suggest that some of the structural and behavioral anomalies, common in patients with *ARX* mutations, are specifically due to alterations in pallial progenitor function. Furthermore, our data demonstrate that some of the neurobehavioral features found in patients with *ARX* mutations may not be due to on-going seizures, as is often postulated, given that epilepsy was eliminated as a confounding variable in these behavior analyses.

Keywords: anxiety, hyperactivity, learning, mouse, socialization

Introduction

Aristaless-Related Homeobox (*ARX*) gene is one of the more commonly mutated genes causing X-linked intellectual disability (XLID; Lin et al. 2009; Shoubridge et al. 2010). Over 44 distinct mutations have been found resulting in a spectrum of phenotypes (Shoubridge et al. 2010). Mutations that lead to a deletion or truncation along with those that reside in the homeodomain cause primarily brain malformation phenotypes, such as X-linked lissencephaly associated with ambiguous genitalia (XLAG), hydranencephaly, and Proud syndrome (agenesis of the corpus callosum, ACC) (Bonneau et al. 1992). Point mutations outside the homeodomain, in nonconserved amino acids of the homeodomain, missense mutations, and poly-alanine track expansion mutations lead to various neurological phenotypes that are mainly characterized by intellectual disability, but frequently also include epilepsy (typically infantile spasms), autism, or dystonia but typically have no structural brain defects (Lafaucheur et al. 1992; Turner et al. 2002). The only phenotype consistently observed in patients with all *ARX* mutations is intellectual disability.

Mice with a germline loss of *Arx* have a thin disorganized cortex, malformed thalamus, major white matter tract defects (corpus callosum and thalamo-cortical), and mislocalization and loss of interneurons in the cortex and striatum (Kitamura et al. 2002). Unfortunately, these mice die shortly after birth precluding behavioral or electrophysiologic phenotyping. In the developing telencephalon, *Arx* is expressed in pallial progenitor cells located in the ventricular zone (VZ) and in subpallial sub-VZ (SVZ) cells, which generate interneurons that populate the cortex, striatum, and hippocampus. The selective removal of *Arx* from interneurons results in what appears to be a structurally normal brain, but similar to the knock-out mouse they have fewer interneurons in the cerebral cortex and hippocampus (Marsh et al. 2009). They also manifest a severe epilepsy phenotype with features overlapping those observed in some patients with *ARX* mutations (Marsh et al. 2009). Hence, it appears that perturbation of the developing interneurons is sufficient to produce an epileptic phenotype that recapitulates the seizures found in patients with *ARX* mutations. Selective removal of *Arx* from the pallial progenitor cells using an shRNA against *Arx* at e13.5 causes the progenitors cells to prematurely exit the cell cycle and the VZ, however, because this was just a partial knock down it is unclear what affect this has on later development of the cortex (Friocourt et al. 2008).

In contrast to mice with a germline loss of *Arx* (Kitamura et al. 2002), mice deficient for *Arx* in cortical interneurons ($Arx^{-/Y}$ $Dlx5/6^{Cre}$ mice) have a normal cortical thickness, indicating an interneuron-independent function of *Arx* on cortical thickness (Marsh et al. 2009). In addition to the complete and conditional knock-out animals, a series of mice with human mutations knocked in have been generated (Kitamura et al. 2009; Price et al. 2009). The knock-in mouse with an altered homeodomain structure had a thinner cortex and was perinatally lethal like the knock-out mouse, whereas the 2 knock-in mutations outside the homeodomain were reported to have a normal cortical thickness recapitulating the genotype–phenotype correlation seen in humans.

To examine the role of *Arx* in cortical development, we mated $Arx^{F/X}$ mice to $Emx1^{Cre}$ mice, which selectively delete *Arx* from the dorsal telencephalon (pallium). These mice have a thin cerebral cortex, similar to the *Arx* knock-out, and are predominantly missing superficial layer neurons, sparing deeper

layer neurons, due to a loss of proliferating intermediate progenitor cells (Colasante et al. 2015). Since the conditional loss of *Arx* in interneurons is associated with an epilepsy phenotype similar to that seen in patients with *ARX* mutations (Marsh et al. 2009), we next sought to determine which characteristics of the human *ARX* patient phenotype might be explained by loss of *Arx* from pallial progenitor cells. Our behavioral and anatomic analysis of the $Arx^{-/Y}$ $Emx1^{Cre}$ mice indicates that ARX plays an essential role in the projection neuron precursors as they relate to behavioral and structural deficits, but apparently not to the epilepsy phenotype.

Materials and Methods

Mice

Arx conditional mutant mice ($Arx^{F/X}$) (Fulp et al. 2008) were maintained on a C57Bl/6 background. To inactivate *Arx* in the dorsal telencephalon specifically during development, $Arx^{F/X}$ heterozygous female mice were crossed with homozygous male $Emx1^{Cre/Cre}$ animals also on a C57Bl/6 background (Jax Mouse Strain 005628). Genotyping to distinguish wild-type, floxed, and cre-positive alleles was performed as described (Jin et al. 2000; Fulp et al. 2008). Mice were maintained at the Children's Hospital of Philadelphia animal facility on a 12 : 12 h light–dark cycle (lights on 0600–1800 h) and ad libitum Lab Diet mouse food 5LG4. All experiments were approved by the Institutional Animal Care and Use Committee of the Children's Hospital of Philadelphia.

EEG Recordings and Analysis

All electrophysiologic studies were conducted as previously described (Marsh et al. 2009). Adult animals at least 3 month olds were used for all EEG recordings. Briefly, under isoflurane anesthesia, 4 electrodes were stereotaxically implanted (3 cortical-left and right frontal, right parietal, and a hippocampal depth) using the coordinates in our previous publication (Marsh et al. 2009). The animals recovered in their home cage for 48 h prior to recordings and then were transferred to the recording cage and recorded with a Triangle Biosystems preamplifer and a Stellate EEG recording system (Natus Technologies) for 48–96 h.

The EEG and video were reviewed manually for the presence of seizures. Background EEG was quantified as previously published (Marsh et al. 2009). Briefly, ten 10-s segments of awake and asleep EEG were randomly selected, but checked for artifact and behavioral state. The awake state was defined as the period when the mouse was moving with hippocampal theta present. In contrast, when the animal was still, head down, and delta dominated the EEG, it was considered asleep. A Fast Fourier Transform (FFT) was calculated for each segment (MATLAB 2010b, Mathworks, Inc., Natick, MA, USA), and the resultant spectrums were quantified by calculating the power in selected bandwidths (Delta 0.1–3.5 Hz, Theta 3.5–8.5 Hz, Alpha 8.5–13 Hz, Beta 13–25 Hz, and Gamma 25–100 Hz) and dividing by total FFT power. The percent power in each bin was averaged across genotype and compared using a Student's *t*-test in Excel (version 12.2.7, Mircosoft). To correct for the 10 comparisons, a difference was considered significant if the *P*-value was <0.005 (the Bonferroni correction). Eight mutant mice and 6 wild-type mice were recorded for 3 days each, but only 4 wild-type and 4 mutant mice were analyzed using the FFT.

Behavioral Studies

Behavioral testing was conducted during the light phase between 1000 and 1800 h, starting at 8 weeks of age and each individual paradigm was separated by at least 2 days. Mice were handled for 5 min each day for 3 days prior to the beginning of testing. Six cohorts of mice were used for behavior testing. Each cohort consisted of at least 2 different litters of mice. See Supplementary Table 1 for a list of the tasks, each cohort of mice performed. The numbers of mice tested for each task are listed below. Only male mice were tested and all cohorts were a mix of mutant mice ($Arx^{F/Y}$ $Emx1^{Cre/Cre}$) and wild-type littermates ($Arx^{X/Y}$ $Emx1^{Cre/Cre}$). Cleaning wipes (PDI Sani-Cloth Plus germicidal disposable cloth) were used to clean equipment between mice. With the exception of grip strength and rota-rod, all paradigms were video-recorded and automatically scored using the ANY-maze software (Stoelting Co., Wood Dale, IL, USA).

Grip Strength

The grip strength of the mice was tested using a grip strength meter (080312-3 Columbus Instruments, Columbus, OH, USA). Each mouse was tested in 6 consecutive trials; the first 3 were for forelimbs, and then 3 more for hindlimbs. The value from each trial was recorded, and the forelimb and hindlimb trials were each averaged and taken as the result for that mouse (Golub and Germann 2001; Fowler et al. 2002; Munn et al. 2011). The results for all mutant mice and their wild-type littermates were compared using a two-tailed unpaired Student's *t*-test in Excel; WT = 13 and Mut = 14.

Rota-Rod

Mice were tested on a rota-rod from Ugo Basile (Model 47600, Comerio, Italy). The mice were tested in groups, 6 at a time for 5 min trials with 5 trials per day for 4 days. The rota-rod was used in acceleration mode, accelerating every 6 s up to 60 rpm. The latency until falling for each mouse was recorded. Between trials the mice were placed back into their home cages (Miwa and Walz 2012; Heyser et al. 2013). Each day, the trials were averaged and the genotypes were compared across 4 days using a repeated-measure ANOVA in Prism (version 5.0, GraphPad, San Diego, CA, USA); WT = 13 and Mut = 14.

Home Cage Activity

Mice were placed in plastic EEG recording boxes (Marsh et al. 2009) with their normal bedding and food and were allowed to acclimate for 2 days before being video-recorded for 3 days. The video was analyzed using an in-house program written in MATLAB that detects movement by subtracting pixels between each video. The pixel counts were averaged over the 3 days of recordings for each genotype. The genotypes were compared using a Student's *t*-test in Excel; WT = 8 and Mut = 8.

Open Field

A 53 × 53 cm plastic box with 22-cm high walls and no top was used in a well-lit room (450 lumens/m^2). The mice were placed in the center of the box and allowed to roam freely in the box for 15 min. The mice were video-recorded and scored using the ANY-maze software. ANY-maze scored a mouse to be in the periphery if it was within 13 cm of the wall of the box. Otherwise they were considered to be in the center of the box (Buschert et al. 2013; Han et al. 2013). The ratio of time in the center to time in the periphery was calculated and averaged. The distance traveled during the test and the number of crossings between the center of the box and the periphery were also calculated and averaged using the ANY-maze software. Genotypes were compared using a two-tailed unpaired Student's *t*-test in Microsoft Excel, version 12.2.7; WT = 20 and Mut = 21.

Light/Dark Box

A 55 × 28 cm plastic box with 22-cm tall walls and divided in half was used. Both sides of the box were accessible by a 7.5 × 7.5 cm door in the middle. One half of the box was clear with no top and the other half was black plastic with a covered top. The mice were placed in the box on the light side and allowed to roam freely for 15 min. The tests were video-recorded and scored using the ANY-maze software (Bale et al. 2000; Bourin and Hascoet 2003). The ratio of time in the light side of the box to time in the dark side was calculated and averaged for each genotype and compared using a two-tailed unpaired Student's *t*-test in Excel. The linear distance the animal traveled during the test and the number of crossings between the two sides was also calculated and analyzed the same way; WT = 17 and Mut = 14.

Marble Burying

A clear plastic cage, 32 × 43 cm, with 19 cm high walls was filled with 5 cm deep corncob bedding evenly covering the bottom. Twenty-four

marbles, spaced 6 cm apart, were placed evenly on top of the bedding. The mice were placed in the box and allowed to roam freely and bury marbles for 30 min. After 30 min, the number of marbles buried at least two-thirds of the marble's depth with bedding was recorded (Deacon 2006; Krass et al. 2010; Chioca et al. 2013). The tests were video-recorded and scored for distance traveled using the ANY-maze software. The number of marbles buried, and the distance traveled was calculated and averaged for each genotype and compared using a two-tailed unpaired Student's *t*-test in Excel; WT = 8 and Mut = 8.

Morris Water Maze

The Morris water maze consists of a 128-cm diameter round plastic tub filled with 21 °C water to within 15 cm of the top of the tub and a 0.5-cm above a square clear plastic platform. A liter of white tempera paint was mixed into the water until it was opaque enough that the edge of the platform could not be seen from the side. Spatial cues were placed around the tub and were not moved for the duration of the experiments. The mice were tested using 4 trials per day for 5 days. The mice were placed in the tank in a different location for each trial and the order of locations was changed each day (Vorhees and Williams 2006; Table 1). In each trial, mice were allowed to swim for up to 60 s before being led to the platform. Once on the platform, the mice were allowed 10 s of observation time. The latency to find the platform (up to 60 s) for each trial was recorded and averaged for each day. The genotypes were compared using a repeated-measures ANOVA in Prism. On the sixth day, a probe trial was performed to test the memory of the location of the platform. In this trial, the platform was removed and the mice swam around the tub, searching for the missing platform for 60 s. The time spent in the quadrant of the tub where the platform had been and in the opposite quadrant was recorded and compared using an unpaired Student's *t*-test. A reversal test was then performed for 5 days following the probe trial. During this test, the platform was placed on the opposite side of the tub and the mice were retrained, with the same protocol of 4 trials a day for 5 days. A reversal probe trial was performed on the sixth day in the same fashion as the first probe trial (Harris et al. 2013). The same statistical analysis was performed for the reversal trials as for the learning test; WT = 20 and Mut = 21.

Contextual Fear Conditioning

Each mouse was placed in a modular test chamber (Model ENV-307W, Med Associates, Inc., Georgia, VT, USA) and allowed to explore the box for 2 h and 30 min before a 2-s foot shock of 1.12 mA was given with a SA shock scrambler (ENV-4145), a digital timer (SG-592), and a 1-Amp power supply (SG-501, Med Associates, Inc., Georgia, VT, USA). The mouse was then left in the box for another 28 s before being removed to its home cage. Twenty-four hours later, the mouse was placed in the same modular test chamber and was video-recorded for 5 min using the ANY-Maze software, which quantified time spent not moving (freezing) (Wood et al. 2005; Cole et al. 2010). The amount of time spent freezing was compared across genotypes using an unpaired Student's *t*-test; WT = 17 and Mut = 14.

Social Choice Test

A social choice apparatus was constructed from the description by Sankoorikal et al. (2006). The bottom of the chamber was covered with bedding and that bedding was changed for each mouse tested. The protocol used to test the mice was the same as the one used in Fairless et al. (2008). Briefly, the mice were first acclimated to the chamber for 10 min. Then, a novel object was added to one tube and a gonadectomized male mouse to the other tube, and the behavior of the test mouse was recorded for 5 min. The tubes were then removed and the behavior of the test mouse while interacting with the gonadectomized mouse was observed for another 5 min, unless the mouse was aggressive in which case both mice were removed immediately. The test mouse was then returned to its home cage. A single novel object was used for all tests and was cleaned, along with the apparatus before each test. Each gonadectomized male was used only once per day. The side of the chamber that had the mouse or the object was alternated between tests (Nadler et al. 2004). The tests were video-recorded and scored using the ANY-maze software. The time spent in the social section, the center, and the nonsocial section was compared using a two-way ANOVA in Prism. The ratio of the amount of time spent within 3 cm of the tube with the mouse (sniffing social tube) versus the time spent within 3 cm of the tube with the object (sniffing object tube) was calculated and averaged for each genotype and compared using a Student's *t*-test in Excel. The number of entries to either the social section of the box (mouse) or the nonsocial section of the box (object) was also calculated and compared across genotypes; WT = 15 and Mut = 18.

Buried Food Test of Olfaction

For 2 days prior to the test each mouse was given a Froot Loop (Kellogg's® Froot Loops® Cereal) in its cage, and the next day the cage was checked to make sure they ate the Froot Loop. Mice were then deprived of food for 24 h. The next day a Froot Loop was buried in 1.5 cm deep bedding in a clean normal mouse cage with nothing else but the top of the cage. A mouse was placed in the cage and the time to dig up the piece of food documented, up to 10 min (Moy et al. 2004; Yang and Crawley 2009). The average time for each genotype was compared using an unpaired Student's *t*-test; WT = 8 and Mut = 8.

In Situ Hybridization

P21 and P30 mice were perfused transcardially with phosphate-buffered saline (PBS) followed by 4% paraformaldehyde (PFA). The brains were removed and post-fixed in 4% PFA overnight at 4 °C. Fixed brains were cryoprotected in 30% sucrose and coronally sectioned at 10 µm. All slides were baked at 65 °C for 20 min, post-fixed in 4% PFA for 10 min, washed in PBS with 0.1% Tween-20 (PBT). The slides were then acetylated for 10 min in 0.1 M TEA (1.86% triethanolamine, 0.4% 10 N NaOH, 0.5% acetic anhydride, and water) and washed in PBT. The glutamate decarboxylase 67 (GAD67) probe (courtesy of Dr N. Tillakaratne; Erlander et al. 1991) was added at 1 : 1000 in prewarmed hybe solution [50% formamide, 5× saline-sodium citrate (SSC), 2% blocking reagent (Roche, Mannheim, Germany; 11096176001), 0.1% Triton, 0.15 CHAPS (3-[(3-cholamidopropyl)dimethylammonio]-1-propanesulfonate), 1 mg/mL tRNA from yeast, 5 mM EDTA, and 50 µg/mL heparin] and incubated overnight at 65 °C. Slides were washed with 5× SSC, then incubated with 1× SSC/50% formamide 30 min at 65 °C, then TNE (10 mM Tris pH 7.5, 500 nM NaCl, 1 mM EDTA, and water) for 10 min at 37 °C, then RNaseA for 30 min at 37 °C and washed with TNE and then at 65 °C with 2× SSC and 0.2× SSC for 20 min, each. Then, the slides were incubated in MABT pH 7.5 (100 mM maleic acid, 150 mM NaCl, 0.1% Tween-20, and water) and blocked in MABT with 2% blocking reagent (Roche) and 20% goat serum for 1 h at room temperature. Slides were incubated overnight at 4 °C in MABT with 2% blocking reagent and 5% goat serum and anti-DIG antibody 1 : 2500 (Roche, 11093274910). The slides were then washed with MABT and NTM (100mM Tris pH 9.5, 100mM NaCl, 50mM MgCl2, and water). The slides were then incubated with 1 mL of BM Purple (Roche, 11442074001) in the dark, overnight at room temperature. The slides were then washed with NTM and PBS, fixed in PFA, dehydrated to 100% ethanol, and mounted with Permount (SP15-500, Fisher Scientific).

Immunohistochemistry

P21 mouse brains were processed as described in the In Situ section above. The brains were cryoprotected in 30% sucrose and cryosectioned coronally at 10 or 16 µm. All slides were baked at 37 °C for 30 min. Two antibodies, somatostatin (SST; Rabbit 3387-1, Epitomics,

Table 1

Cohorts of mice used in behavior experiments and order of behavior tests

Cohort	Number of mice	Order of behavior tests
1	WT = 3 Mut = 4	Grip strength, rota-rod, open field, water maze
2	WT = 10 Mut = 8	Grip strength, rota-rod, open field, water maze
3	WT = 13 Mut = 9	Light/dark box, open field, water maze, fear conditioning
4	WT = 4 Mut = 5	Light/dark box, buried food, social choice, fear conditioning
5	WT = 11 Mut = 13	Buried food, social choice
6	WT = 8 Mut = 8	Buried food

Burlingame, CA, USA; 1 : 50) and parvalbumin (Parv; Mouse MAB1572, Millipore, Billerica, CA, USA; 1 : 100), were used to assess for changes in interneuron subtypes. For the *Sst* antibody, antigen retrieval was performed in citric acid-based antigen unmasking solution (H-3300, Vector Laboratories, Burlingame, CA, USA) autoclaved at 105 °C for 20 min. For the *Parv* antibody, the MOM blocking reagent (FMK-2201, Vector Laboratories) was used for 30 min followed by blocking for 30 min with 10% normal goat serum (Sigma) in TBST (TBS with 0.5% triton) all at room temperature. After antigen retrieval, SST sections were blocked for 30 min at room temperature with 0.5% normal goat serum (Sigma) in TBST. Anti-*Parv* primary was diluted in 1% normal goat serum in TBST, and Anti-*Sst* was diluted in 0.5% normal goat serum in TBST and incubated on slides overnight at 4 °C. The secondary antibodies used were a biotinylated goat anti-mouse (BA-9200, Vector Laboratories, 1 : 300) and biotinylated goat anti-rabbit (BA-1000, Vector Laboratories, 1 : 300), diluted in TBST, and placed on slides for 30 min at room temperature. The biotinylated secondary antibodies were subsequently incubated with ABC kit mix (PK-6100, Vector Laboratories) in PBS for 30 min and then ImmPACT DAB for 2 min (SK-4105, Vector Laboratories). Slides were counterstained with hematoxylin, dehydrated, and mounted with Permount. Stained sections were viewed on a Leica DM6000B equipped with a Leica DFC360FX digital camera. 10× images were taken of the entire cortex for each section and then stitched together using Fiji version ImageJ 1.45b.

Nissl Staining

Cresyl Violet acetate (C5042, Sigma-Aldrich) (0.1 g) was mixed with 100 mL of distilled water. To each 10 mL of Cresyl Violet acetate solution, 50 µL of 15% glacial acetic acid was added and the solution was filtered to make Nissl stain. Cryosections were covered in Nissl stain for 10 min and then washed 2 times with distilled water. The sections were destained by dipping them once in acid alcohol (50% ethanol/50% distilled water with 0.1% HCl). Slides were mounted with Flouromount-G (0100-01, SouthernBiotech) and imaged the same as the immunohistochemistry sections.

Cell Counting

For the GAD67 counts, an 1-mm area of the cortex from the pial surface to the white matter directly above the hippocampus (2 mm posterior to bregma) and 2 mm from the medial edge of the cortex was counted. For the basolateral amygdala counts, all the Nissl-stained neurons in the basolateral amygdala (2.1 mm posterior to bregma) were counted. Cell counts were averaged for each genotype and compared using an unpaired Student's *t*-test.

Magnetic Resonance Imaging

Adult mice brains were processed as described above and then post-fixed in 4% PFA for 2 weeks. Prior to MRI, the samples were transferred to a PBS 1× solution containing 0.2 mM Gd-DTPA (gadopentetic acid) (J140 Omniscan GE Healthcare). At the time of scanning, the samples were removed from the PBS/Gd-DTPA solution, rinsed with pure PBS, and introduced in a short 11-mm glass tube containing Fomblin (317993 Sigma-Aldrich) to provide a susceptibility match and a black background for the images. Bubbles were carefully removed by tapping gently on the tube. An inverted Pasteur pipette was inserted on top of the brain to maintain the tissue immersed in the Fomblin. MRI was performed at 9.4 T in a vertical bore magnet (Avance III Bruker Biospin, Inc.) using the micro 2.5 self-shielded gradients (2.5 G/cm/A) and a 15-mm RF coil. The image acquisition and reconstruction was performed with the Paravision software 5.1 (Bruker Biospin, Inc.). The temperature of the sample was maintained at 37 °C. Diffusion tensor images and T_2-weighted 3D images of the brain tissue were obtained sequentially with the DTIEpi 30 directions and the 3D turboRARE Bruker protocols, respectively. The following conditions were used: for the DTI, field of view (FOV) 20 × 12.8 × 10 mm, data size (SI) 128 × 80 × 64, which results in a resolution of 160 m^3, number of averages (NEX) 2, repetition time (TR) 1250 ms, echo spacing (Te) 26 ms, 8 segments, bandwidth 300 kHz, diffusion gradients 3 ms, diffusion gradient separation 7.53 ms, 30 directions, 5 A0 images, and a *B*- value of 1500 s mm^{-2}. The duration of the acquisition was 12 h 26 min. For the 3D rare, the parameters were FOV 19.2 × 12.8 × 9.6 mm, SI 256 × 176 × 128, giving a resolution of 75 m^3, 5 NEX, TR 1500 ms, Te 13 ms, echo train 8, which results in an average echo time of 39 ms and a 5-h long experiment. To analyze the T_2-weight images for volume data on specific brain regions we used a registration-based segmentation method to extract various structures in T_2-weight MR images of mouse brains. A mouse brain atlas with accompanying labels of structures of interest was registered to the target image. We adapted the mouse atlas from Johns Hopkins University, which is available to the public (http://cmrm.med.jhmi.edu/). Registration was aligned followed by nonrigid diffeomorphic warping using Advanced Normalization Tools (ANTs), which is an open-source software freely available online. The labels were also transformed to the target space by the same warping and thus completed the segmentation.

Results

$Arx^{-/Y}$ $Emx1^{Cre}$ Mutant Mice Have Normal Numbers of Interneurons

We previously found that $Arx^{-/Y}$ $Emx1^{Cre}$ mice have reduced numbers of upper cortical layer neurons with relative sparing of neurons in the deeper layers (Colasante et al. 2015). *Arx* expression was preserved in the developing ventral telencephalon and in the interneurons migrating from the ganglionic eminence to the cortex (Colasante et al. 2015). Several studies have found that changes in the development of cortical excitatory neurons can affect interneuron migration into the cortex (Sessa et al. 2010; Lodato et al. 2011). Therefore, to confirm that cortical interneurons were not adversely affected by the loss of upper layer neurons we first assessed the total number of interneurons using a GAD67 in situ hybridization probe on sections from brains of P21 $Arx^{-/Y}$ $Emx1^{Cre}$ (mutant) mice and their wild-type littermates ($Arx^{X/Y}$ $Emx1^{Cre}$). Similar numbers of interneurons were found in the mutant brains when compared with wild-type brains (Fig. 1*A*,*B*; WT = 137.3 ± 5.84 and Mut = 124 ± 2.65; $n = 3$ for each; $P = 0.1359$).

We next sought to exclude the possibility that while the total number of interneurons was unchanged, subtypes of interneurons were disproportionately represented (Azim et al. 2009). Labeling for 2 interneuron subtypes, Parv and SST, which together mark 50–70% of all cortical interneurons (Xu et al. 2010; Rudy et al. 2011), revealed both types to be similarly represented (Fig. 1*A*: Parv WT = 50 ± 5 and Mut = 53 ± 2; $n = 3$ for each; $P = 0.6575$; SST WT = 37 ± 7.23 and Mut = 29 ± 2.89; $n = 3$ for each; $P = 0.3897$). Thus, both the total number and representative subtypes of interneurons were unaltered by the loss of *Arx* from the dorsal telencephalon.

$Arx^{-/Y}$ $Emx1^{Cre}$ Mice Do Not Have Seizures

Patients and mice with *ARX/Arx* mutations have seizures as a principle feature. The conditional loss of *Arx* from developing interneurons in the ventral telencephalon ($Arx^{-/Y}$ $Dlx5/6^{Cre}$) results in a severe seizure phenotype (Marsh et al. 2009). Furthermore, mice with a poly-alanine track expansion mutation or with a point mutation in the homeobox also have seizures (Kitamura et al. 2009; Price et al. 2009). To determine if the loss of *Arx* from the cortical projection neuron progenitor pools ($Arx^{-/Y}$ $Emx1^{Cre}$ mice) is also associated with seizures, video-EEGs were recorded for up to 96 h following our previously published protocol (Marsh et al. 2009). Review of up to 96 h of EEG and video recordings from 8 mutant mice and 6 control animals revealed no seizures in the either the mutant

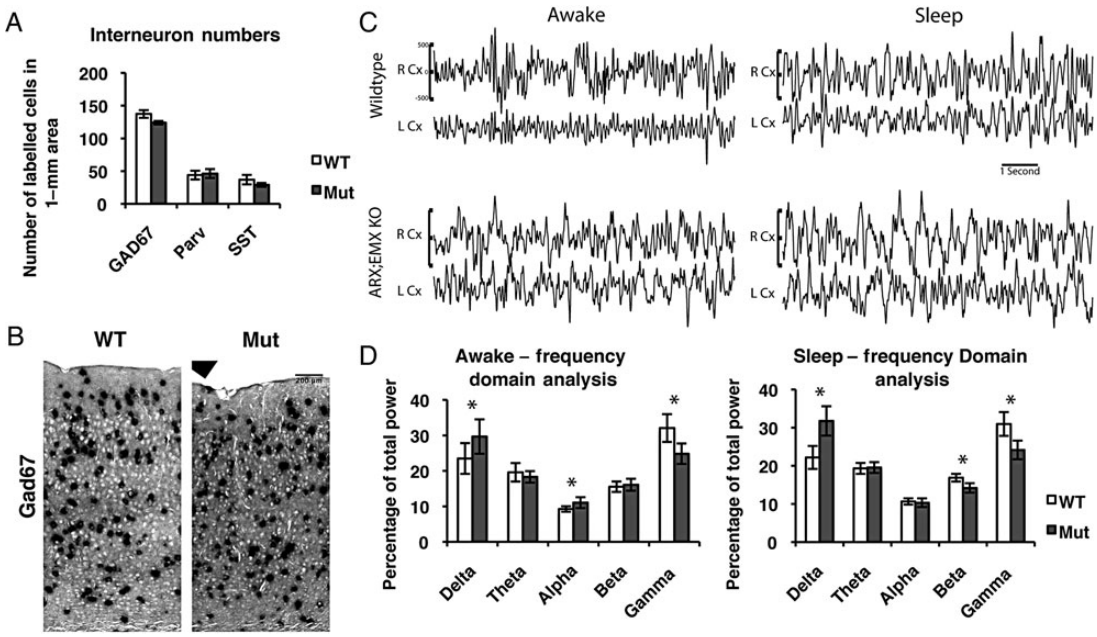

Figure 1. *Arx*$^{-/Y}$ *Emx1-Cre* mice do not have seizures and have normal interneuron numbers. (*A*) Quantifications of interneurons in a 1-mm bin of cortex from ventricular to pial surface from in situ hybridizations of GAD67 and immunofluorescence staining of Parv and SST on adult brain sections, showing no difference in the total number of interneurons (GAD67; WT = 137.3 ± 5.84 and Mut = 24 ± 2.65; $n = 3$ for each; $P = 0.1359$) and no change in the number of interneurons of 2 subtypes (Parv; WT = 50 ± 5 and Mut = 53 ± 2; $n = 3$ for each; $P = 0.6575$; and SST; WT = 37 ± 7.23 and Mut = 29 ± 2.89; $n = 3$ for each; $P = 0.3897$). Error bars correspond to SE. (*B*) GAD67 in situ hybridizations on cryosections of P21 brains of wild-type (Arx$^{X/Y}$ Emx1-Cre) and mutant (Arx$^{F/Y}$ Emx1-Cre) brains. Section of the cortex just above the hippocampus from pial surface (top) to white matter (bottom). (*C*) Samples of cortex recordings for *Arx*$^{-/Y}$ *Emx1-Cre* mice (Mut) and their control wild-type littermates (*Arx*$^{X/Y}$ *Emx1-Cre*), which showed no seizure activity. (*D*) Quantifications of EEGs of the cortex by FFT on both Awake and Sleep segments for wild-type and mutant mice (Awake—Delta: WT = 23.50 ± 4.34 and Mut = 29.69 ± 4.85, $P = 0.0036$; Theta: WT = 19.61 ± 2.60 and Mut = 18.32 ± 1.63, $P = 0.1894$; Alpha: WT = 9.28 ± 0.77 and Mut = 11.06 ± 1.53, $P = 0.0017$; Beta: WT = 15.54 ± 1.46 and Mut = 16.11 ± 1.68, $P = 0.4199$; Gamma: WT = 32.08 ± 3.92 and Mut = 24.83 ± 2.89, $P = 9.1 \times 10^{-6}$; Sleep—Delta: WT = 22.19 ± 3.84 and Mut = 31.77 ± 3.84, $P = 2.3 \times 10^{-8}$; Theta: WT = 19.32 ± 1.42 and Mut = 19.55 ± 1.41, $P = 0.7178$; Alpha: WT = 10.65 ± 0.83 and Mut = 10.32 ± 1.13, $P = 0.4597$; Beta: WT = 16.88 ± 1.00 and Mut = 14.20 ± 1.24, $P = 9.2 \times 10^{-7}$; Gamma: WT = 30.96 ± 3.11 and Mut = 24.16 ± 2.46, $P = 4.7 \times 10^{-7}$; WT $n = 6$ and Mut $n = 4$).

or control mice. However, there were differences that were observed in the EEG (Fig. 1*C*). Qualitatively, the EEG appeared to be slower in the *Arx*$^{-/Y}$ *Emx1*^{Cre} mice than the wild-type mice (Fig. 1*C*). To confirm our visual interpretation, we performed FFTs on randomly selected awake and sleep EEG segments in the cortex from 6 control and 4 mutant mice. An increase in Delta (Awake: WT = 23.50 ± 4.34 and Mut = 29.69 ± 4.85, $P = 0.0036$; Sleep: WT = 22.19 ± 3.84 and Mut = 31.77 ± 3.84, $P = 2.3 \times 10^{-8}$) and a decrease in Alpha or Beta (Awake—Alpha: WT = 9.28 ± 0.77 and Mut = 11.06 ± 1.53, $P = 0.0017$; Sleep—Beta: WT = 16.88 ± 1.00 and Mut = 14.20 ± 1.24, $P = 9.2 \times 10^{-7}$) and Gamma (Awake: WT = 32.08 ± 3.92 and Mut = 24.83 ± 2.89, $P = 9.1 \times 10^{-6}$; Sleep: WT = 30.96 ± 3.11 and Mut = 24.16 ± 2.46, $P = 4.7 \times 10^{-6}$; WT $n = 6$ and Mut $n = 4$) power were present during both sleep and awake states (Fig. 1*D*). Similarly, results were seen in the FFTs for the hippocampal recordings (Supplementary Fig. 1*A*,*B*). Interestingly, this change in EEG frequency content is the opposite from the *Arx*$^{-/Y}$ *Dlx5/6*^{Cre} mice, which had an increase in faster (Beta and Gamma) activity (Marsh et al. 2009).

Arx$^{-/Y}$ *Emx1*^{Cre} *Mutant Mice Have Normal Spatial Learning and Memory*

An invariant feature among males with an *ARX* mutation is a severe intellectual disability (Shoubridge et al. 2010). Normal learning and memory in mice are often used as a corollary of normal intellectual ability in people. To investigate whether the *Arx*$^{-/Y}$ *Emx1*^{Cre} mice had normal learning and memory, we performed several tests. Prior to performing these tasks, physical strength and coordination defects were evaluated and excluded. Grip strength and rota-rod testing revealed no differences between the *Arx*$^{-/Y}$ *Emx1*^{Cre} mice and their wild-type littermates (Supplementary Fig. 2*A*,*B*; grip strength: forelimb: WT = 0.042 ± 0.0033, $n = 13$ and Mut = 0.052 ± 0.0053, $n = 12$; $P = 0.1030$; hindlimb: WT = 0.079 ± 0.0055, $n = 13$ and Mut = 0.082 ± 0.0044, $n = 12$; $P = 0.3447$; rota-rod: WT $n = 13$ and Mut $n = 12$; $P = 0.0801$). Thus, no motor deficits were uncovered, suggesting that the mutant mice should have normal physical capabilities.

Once a motor abnormality was excluded, the Morris water maze test was performed to assess spatial learning and memory. The mice were first trained with spatial cues around the tank and the platform hidden. There was no difference in learning the task as both mutant mice and wild-type littermates located the platform in similar times each day of training (Fig. 2*A*; WT $n = 20$ and Mut $n = 21$; $P = 0.0669$). Next, memory for the platform location was probed by recording the time spent in the original quadrant of the platform after the platform was removed (Fig. 2*B*). In addition, there was no difference found between the mutant and wild-type mice (Fig. 2*B*: time in platform quadrant: WT = 22.8 ± 1.47 s and Mut = 25.6 ± 1.97 s; $P = 0.271$; time in opposite quadrant: WT = 9.61 ± 1.07 s, $n = 20$ and Mut = 7.7 ± 1.28 s, $n = 21$; $P = 0.256$). Finally, reversal learning and memory testing, which is a more sensitive indicator to changes in cortical function, were tested by relocating the platform to the opposite side of the tank. No differences were noted in this measure of cortically mediated learning (Fig. 2*C*; WT $n = 20$ and Mut $n = 21$;

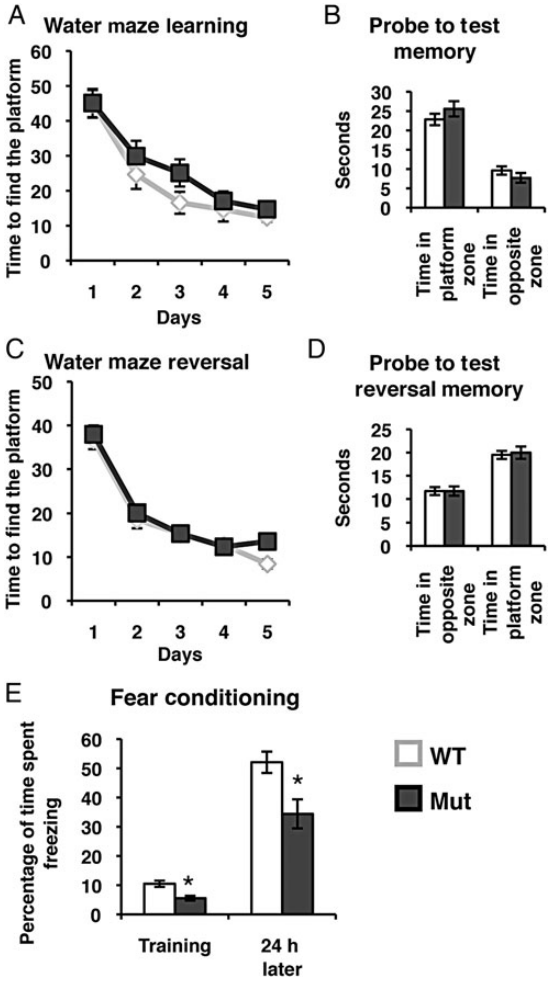

Figure 2. *Arx*$^{-/Y}$ *Emx1-Cre* mice have normal spatial learning and memory, but impaired fear-based memory. (*A*) Mutant mice and wild-type littermates were trained in the Morris water maze for 5 days and the mutants learned how to reach the platform just as quickly as their wild-type littermates (WT $n = 20$ and Mut $n = 21$; $P = 0.0669$). (*B*) On day 6 with the platform removed the mutant mice spent just as much time as their wild-type littermates in the correct quadrant showing that they remembered where the platform was located (time in platform quadrant: WT = 22.8 ± 1.47 s and Mut = 25.6 ± 1.97 s; $P = 0.271$; time in opposite quadrant: WT = 9.61 ± 1.07 s, $n = 20$ and Mut = 7.7 ± 1.28 s, $n = 21$; $P = 0.256$). (*C*) The reversal learning of the mice was then tested by retraining them for another 5 days with the platform on the opposite quadrant of the tank. The mutant mice relearned the task just as well as their wild-type littermates (WT $n = 20$ and Mut $n = 21$; $P = 0.1545$). (*D*) On day 12, the platform was again removed and the time the mice spent in each quadrant was recorded. The mutant mice spent just as much time in the new platform quadrant as their wild-type littermates (time in platform quadrant: WT = 19.5 ± 0.87 s and Mut = 19.9 ± 1.33 s; $P = 0.762$; time in opposite quadrant: WT = 11.7 ± 0.85 s, $n = 20$ and Mut = 11.7 ± 1.02 s, $n = 21$; $P = 0.997$). (*E*) Contextual fear conditioning was used to evaluate fear learning in wild-type and mutant mice. During a 3-min training period, the mice were given a foot shock and the amount of time spent freezing was recorded. Twenty-four hours later, the mice were re-exposed to the context where they were given the foot shock and the amount of time they spent freezing over a 5-min period was recorded. Mutant mice spent significantly less time freezing when compared with their wild-type littermates both in the training period and during testing, so therefore they did learn this task (percentage of time spent freezing training: WT = 10.5 ± 1.06, $n = 17$ and Mut = 5.57 ± 0.82, $n = 14$; $P = 0.00099$; percentage of time spent freezing testing: WT = 52.1 ± 3.65, $n = 17$ and Mut = 34.4 ± 4.99, $n = 14$; $P = 0.0086$). Error bars are SE.

$P = 0.1545$) or memory (Fig. 2*D*: time in platform quadrant: WT = 19.5 ± 0.87 s and Mut = 19.9 ± 1.33 s; $P = 0.762$; time in opposite quadrant: WT = 11.7 ± 0.85 s, $n = 20$ and Mut = 11.7 ± 1.02 s, $n = 21$; $P = 0.997$). Thus, by the highly standardized and accepted Morris water maze paradigm, the *Arx*$^{-/Y}$ *Emx1*^{Cre} mice exhibit normal spatial learning, memory, and reversal learning.

Arx$^{-/Y}$ *Emx1*^{Cre} *Mutant Mice Have Normal Fear Memory, But Are Hyperactive*

In some mutant mouse strains, hippocampal-based spatial learning and memory can be normal despite alterations in other forms of learning such as fear-conditioning learning because the hippocampus is not as involved in this type of learning (Angelo et al. 2003; d'Isa et al. 2011; Albarran-Zeckler et al. 2012). To test whether the *Arx*$^{-/Y}$ *Emx1*^{Cre} mutant mice had a learning and memory deficit independent of spatial learning, we tested the animals in a conditioned fear-learning task. The mutant mice spent significantly less time freezing than their wild-type littermates did both during the training session and during the testing session (Fig. 2*E*: percentage of time spent freezing training: WT = 10.5 ± 1.06, $n = 17$ and Mut = 5.57 ± 0.82, $n = 14$; $P = 0.00099$; percentage of time spent freezing testing: WT = 52.1 ± 3.65, $n = 17$ and Mut = 34.4 ± 4.99, $n = 14$; $P = 0.0086$). This suggests that the mutant mice are hyperactive; a finding confirmed by the longer distances traveled by the mutant mice than their wild-type littermates during the testing session (Supplementary Fig. 4*A*: distance traveled: WT = 2.43 ± 0.42 m, $n = 17$ and Mut = 4.00 ± 0.49 m, $n = 14$; $P = 0.0217$). The ratio of the percentage of time spent freezing during the training session versus the testing session indicated that the mutant mice learn the contextual fear conditioning just as well as their wild-type littermates (Supplementary Fig. 4*B*: ratio of percentage of time spent freezing training/testing: WT = 5.36 ± 0.43, $n = 17$ and Mut = 6.80 ± 1.31, $n = 14$; $P = 0.3097$).

Arx$^{-/Y}$ *Emx1*^{Cre} *Mutant Mice Are Less Anxious, More Exploratory, and More Active Than Wild-Type Mice*

Surprisingly, no learning deficit was uncovered but there was a suggestion of a more active state; therefore, we further examined the mutants exploratory and anxiety behaviors. To evaluate the anxiety level of the *Arx*$^{-/Y}$ *Emx1*^{Cre} mutant, mice open field and light/dark box tests were used. For the open field test, mice with a higher ratio of the time spent in the center to time spent in the periphery of the chamber are considered to have a low anxiety-like or anxiolytic phenotype. Mutant mice appeared anxiolytic as they spent significantly more time in the center of the box compared with their wild-type littermates (Fig. 3*A*: WT = 0.170 ± 0.019, $n = 20$ and Mut = 0.229 ± 0.020, $n = 21$; $P = 0.0405$). For the light/dark box, testing the ratio of time spent on the light side of the box compared with that on the dark side of the box was used as a measure of anxiety. In addition, the mutant mice spent significantly more time on the light side when compared with their wild-type littermates, suggesting a reduced anxiety-like phenotype (Fig. 3*C*: WT = 0.891 ± 0.118, $n = 17$ and Mut = 1.61 ± 0.202, $n = 14$; $P = 0.00204$).

Both the open field and light/dark box tests can also be used to quantify the activity level of mutant mice. In both, the mutant mice traveled further than their wild-type littermates indicating a higher activity level in the mutant mice (Fig. 3*B*,*D*: open field: WT = 65.9 ± 3.02 m, $n = 20$ and Mut = 77.6 ± 3.79 m, $n = 21$; $P = 0.0201$; light/dark box: WT = 12.2 ± 0.867 m, $n = 17$ and Mut = 20.2 ± 1.13 m, $n = 14$; $P = 0.000007$). Similarly, the mutant mice more frequently crossed between the light and dark side of the box and between the center and the periphery of the open field, which also indicates higher activity (Supplementary Fig. 3*A*,*B*:

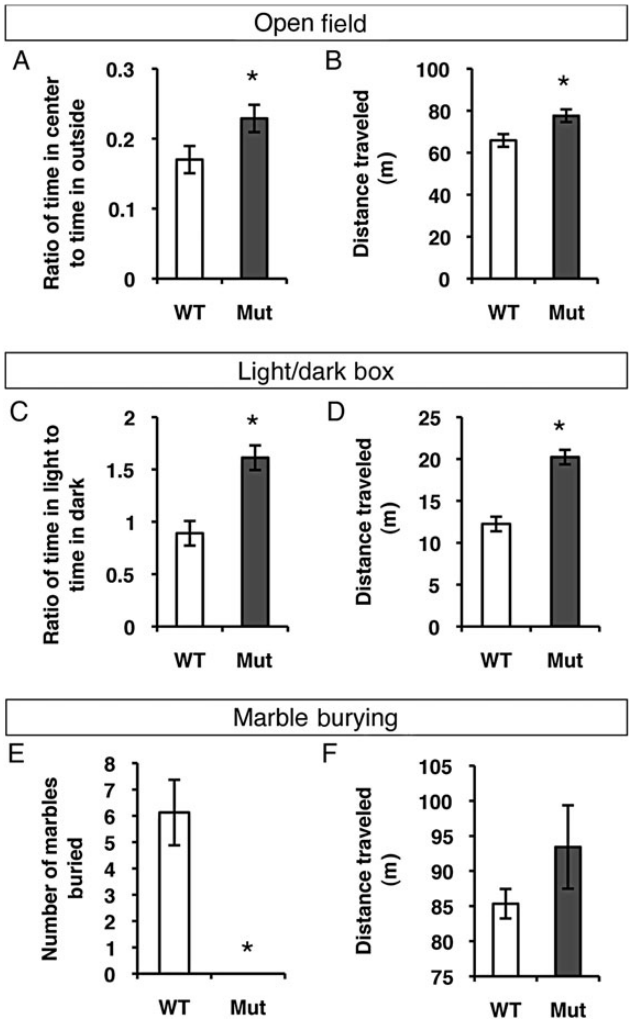

Figure 3. *Arx*$^{-/Y}$ *Emx1-Cre* mice are less anxious and more active than wild-type mice. (*A*) In the open field test, the ratio of time spent in the center to time spent in the outside area of the box was used as a measure of anxiety. The mutant mice spent more time in the center of the box than their wild-type littermates, indicating they are less anxious (WT = 0.170 ± 0.019, $n = 20$ and Mut = 0.229 ± 0.020, $n = 21$; $P = 0.0405$). (*B*) The linear distance traveled by the mice during their 15-min testing period was calculated as a measure of their activity level. The mutant mice traveled further than their wild-type littermates during the open field test, indicating that they are hyperactive (WT = 65.9 ± 3.02 m, $n = 20$ and Mut = 77.6 ± 3.79 m, $n = 21$; $P = 0.0201$). (*C*) For the light/dark box assay, the ratio of time spent in the light side of the box to time spent in the dark side of the box was used as a measure of anxiety. The mutant mice spent more time in the light side of the box than their wild-type littermates, indicating that they are less anxious (WT = 0.891 ± 0.118, $n = 20$ and Mut = 1.61 ± 0.202, $n = 21$; $P = 0.00204$). (*D*) The linear distance traveled by the mice during their 10-min testing period was calculated as a measure of their activity level. The mutant mice traveled further than their wild-type littermates during the light/dark box test, again indicating that they are hyperactive (WT = 12.2 ± 0.867 m, $n = 20$ and Mut = 20.2 ± 1.13 m, $n = 21$; $P = 0.000007$). (*E*) The number of marbles buried in the Marble Burying assay was used as a measure of anxiety with increased burying meaning increased anxiety (WT = 6.13 ± 1.25, $n = 8$ and Mut = 0 ± 0, $n = 8$; $P = 0.00759$). (*F*) The amount of distance traveled by the mice during the 30-min testing period was used as a measure of activity level (WT = 85.34 ± 2.10 m, $n = 8$ and Mut = 93.42 ± 5.94 m, $n = 8$; $P = 0.2322$). Error bars are SE.

open field: WT = 117 ± 6, $n = 20$ and Mut = 158 ± 8, $n = 21$; $P = 0.0000863$; light/dark box: WT = 28 ± 1, $n = 17$ and Mut = 40 ± 4, $n = 14$; $P = 0.00143$). However, the mutant mice displayed normal activity levels in home cage recordings, so they appear to be more active only in novel environments (Supplementary Fig. 2*C*: WT = 13.75 ± 1.73 Δ pixels/frame, $n = 8$ and Mut = 12.59 ± 1.84 Δ pixels/frame, $n = 8$; $P = 0.5191$).

Since our data suggests that the *Arx*$^{-/Y}$ *Emx1*^{Cre} mice are both less anxious and more active in both the open field and the light/dark box tests, we wanted to determine whether the increased activity was confounding our anxiety test results. Therefore, we performed a marble burying test, another anxiety test, but one in which less activity constitutes lower anxiety (Thomas et al. 2009). We found that the mutant mice buried significantly fewer marbles than the wild-type animals (Fig. 3*E*: WT = 6.13 ± 1.25, $n = 8$ and Mut = 0 ± 0, $n = 8$; $P = 0.00759$), yet they were still hyperactive based on distance traveled in the novel cage (Fig. 3*F*: WT = 85.34 ± 2.10 m, $n = 8$ and Mut = 93.42 ± 5.94 m, $n = 8$; $P = 0.2322$), similar to the open field and light dark box. This indicates that although still hyperactive in a novel environment, they were less anxious than their wild-type littermates. Taken together, the data suggest that the anxiety and hyperactivity phenotypes are separable and the *Arx*$^{-/Y}$ *Emx1*^{Cre} mice are both less anxious and hyperactive when compared with their wild-type littermates.

Arx$^{-/Y}$ *Emx1*^{Cre} *Mutant Mice Have Social Deficits*

One of the core symptoms of autism is abnormal social interactions (Crawley 2007; Silverman et al. 2010). To test for the mice for "social" deficits, we performed the social choice task (Crawley 2007; Silverman et al. 2010). In the social choice task, the test mouse is given a choice between a novel object and novel mouse. As mice are normally social animals, they should typically spend more time exploring a novel mouse than a novel object. Therefore, we compared the time spent in the area of the novel mouse (social), the time spent in the center, and the time in the section with the novel object (nonsocial) (Sankoorikal et al. 2006; Fairless et al. 2008). The *Arx*$^{-/Y}$ *Emx1*^{Cre} mutant mice appear to have a socialization deficit as they spent significantly less time in the social section of the box (Fig. 4*A*; time spent in social section: WT = 142.07 ± 8.54 s, $n = 15$ and Mut = 111.37 ± 4.28 s, $n = 18$; $P < 0.001$). In addition, the mutant mice entered the social section of the box significantly fewer times when compared with the wild-type mice (Fig. 4*B*; WT = 2.97 ± 0.50, $n = 15$ and Mut = 1.44 ± 0.14, $n = 18$; $P = 0.00952$). Similarly, mutant mice spent significantly less time sniffing around the novel mouse versus the novel object than their wild-type littermates did (Fig. 4*B*; WT = 4.53 ± 0.80, $n = 15$ and Mut = 2.15 ± 0.18, $n = 18$; $P = 0.01379$).

Since the *Arx*$^{-/Y}$ *Emx1*^{Cre} mutant mice have smaller olfactory bulbs (Colasante et al. 2015), the olfactory ability of the mice was tested using the buried food test in order to rule out the possibility that reduced olfactory ability was confounding the social choice test. Both the mutant mice and their wild-type littermates found the buried Froot Loop in similar amounts of time, showing that the mutants have normal olfactory skills (Fig. 4*C*; WT = 143.38 ± 34.86 s and Mut = 242.13 ± 79.60 s, $n = 8$ for each; $P = 0.2834$); in addition, the *Arx*$^{-/Y}$ *Emx1*^{Cre} mutant mice were able to breed and gain weight normally suggesting they have normal olfactory abilities (data not shown).

Arx$^{-/Y}$ *Emx1*^{Cre} *Mutant Mice Have Smaller Cerebral Cortices, Amygdalas, and White Matter Tracts*

In addition to the neurocognitive and behavioral deficits, patients with various *ARX* mutations exhibit, and structural defects

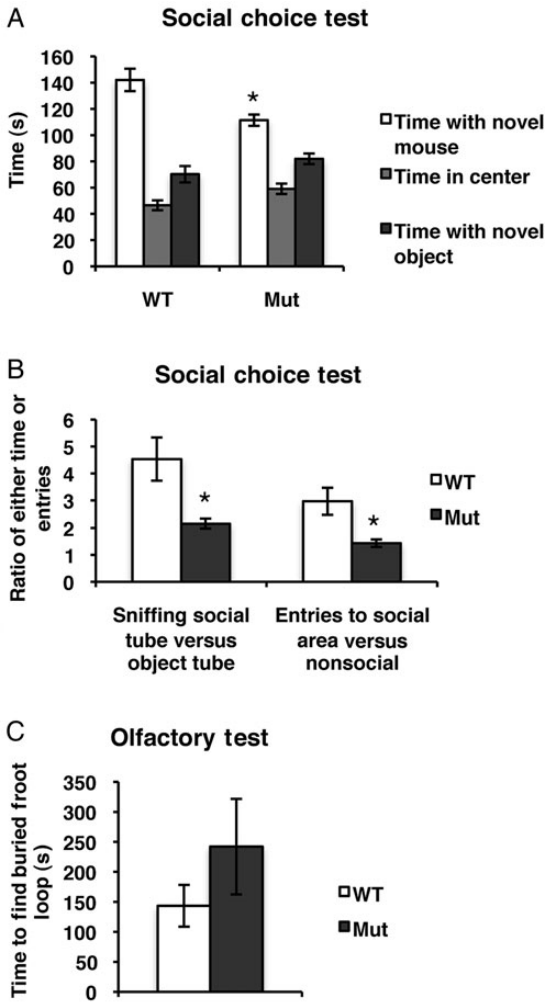

Figure 4. *Arx*$^{-/Y}$ *Emx1-Cre* mice have social deficits. (*A*) The social abilities of mutant and wild-type mice were assessed using the social choice test. The time spent in the novel mouse section (social), the center of the box, and the novel object section (nonsocial) were compared using a two-way ANOVA. The mutant mice spent significantly less time in the social section of the box than their wild-type littermates did (time spent in social section: WT = 142.07 ± 8.54 s, $n = 15$ and Mut = 111.37 ± 4.28 s, $n = 18$; $P < 0.001$). (*B*) The mutant mice spent significantly less time sniffing the novel mouse tube than their wild-type littermates did, compared with the object tube (sniffing: WT = 4.53 ± 0.80, $n = 15$ and Mut = 2.15 ± 0.18, $n = 18$; $P = 0.01379$). The mutant mice also entered the social section of the box few times when compared with the nonsocial section than their wild-type littermates did (entries: WT = 2.97 ± 0.50, $n = 15$ and Mut = 1.44 ± 0.14, $n = 18$; $P = 0.00952$). (*C*) To assess the olfactory ability of the mice, the buried food test was used. If the mice have normal olfactory abilities, they should be able to find the Froot Loop buried in the bedding. Both the mutant mice and their wild-type littermates were equally capable of finding the Froot Loop (WT = 143.38 ± 34.86 s and Mut = 242.13 ± 79.60 s, $n = 8$ for each; $P = 0.2834$). Error bars are SE.

such as lissencephaly, ACC, and microcephaly are present in many patients (Suri 2005; Friocourt et al. 2006; Gecz et al. 2006). In an effort to begin linking the structural defects with the neurocognitive deficits, we examined regional size variation and connectivity. Using structural MRI in fixed *Arx*$^{-/Y}$ *Emx1*^{Cre} and wild-type mouse brains, the volume of various brain structures was calculated (Fig. 5). As observed in Nissl-stained sections, the cerebral cortical volume was significantly smaller in the mutant mouse (Colasante et al. 2015) (Fig. 5*A*,*C*,*E*). The MRIs also revealed the corpus callosum and anterior commissure to be significantly reduced in volume, as is also found in patients with various *ARX* mutations (Proud et al. 1992; Bonneau et al. 2002; Marsh et al. 2009) (Fig. 5*A*,*C*–*E*). However, analysis of the MRIs also revealed that the amygdala volume was significantly smaller in the mutant mice (Fig. 5*E*). The reduction in amygdala volume could be due to loss of inputs, but it is also possible that there are developmental changes to the amygdala in the *Arx*$^{-/Y}$ *Emx1*^{Cre} mice since both *Arx* and *Emx1* are expressed there (Puelles et al. 2000; Medina et al. 2004; Poirier et al. 2004; Remedios et al. 2007). To confirm this finding, we counted neurons in the basolateral amygdala in Nissl-stained sections and found that the number of neurons was reduced (Fig. 6*C*; WT = 1118 ± 124 and Mut = 891 ± 152, $n = 3$ for each; $P = 0.01952$). Interestingly, the behavioral phenotypes of decreased anxiety and loss of fear memory have been hypothesized to represent amygdala dysfunction (Phillips and LeDoux 1992; Grillon et al. 1996; Tottenham et al. 2010; Schienle et al. 2011). Combining the MRI volume changes with the loss of cells in the basolateral amygdala suggests that amygdala dysfunction could explain at least part of the *Arx*$^{-/Y}$ *Emx1*^{Cre} behavioral phenotype. Over all, the MRI data are consistent with the hypothesis that the *Arx*$^{-/Y}$ *Emx1*^{Cre} mutant mice have a long-range connectivity defect. Unexpectedly, the thalamus was also significantly smaller in the mutant mice even though the *Cre* is not expressed in the diencephalon, suggesting a possible corticothalamic connectivity defect (Fig. 5*E*) that could contribute to the abnormal behaviors found in these mice.

Discussion

Loss of *Arx* in dorsal progenitors resulted in structural, functional, and behavioral deficits in the *Arx*$^{-/Y}$ *Emx1*^{Cre} mice. Specifically, we demonstrated that disruption of both local superficial cortical connections, long-range connections between hemispheres and within limbic regions results in a hyperactive and less anxious mouse that socializes poorly. By comparing the deficits in the *Arx*$^{-/Y}$ *Emx1*^{Cre} mice with those of the previous *Arx* mutant mice and the clinical phenotype of *ARX* patients, we can begin to shed some insights on the possible function of different cortical regions, connections, and the role of seizures in various behaviors seen in the *Arx*/*ARX* mice and possibly patients.

The pattern of behaviors and lack of seizures observed in the *Arx*$^{-/Y}$ *Emx1*^{Cre} mice was somewhat surprising given the prototypical phenotype of *ARX* patients; intractable seizures and intellectual disability. The results of the behavioral studies were interpreted with reference to the anatomical and cellular changes observed as well as the phenotype of the other *Arx* models that have been generated. The anatomical changes in the mice recapitulated, to a degree, the findings in the germline deletion of *Arx* created by the Kitamura Laboratory. Both the *Arx* knock-out and our *Arx*$^{-/Y}$ *Emx1*^{Cre} animals developed a thin cortex due to decreased cortical progenitor proliferation during development (Kitamura et al. 2002). Both our previous work (Colasante et al. 2015) and that of others (Friocourt et al. 2008) demonstrated that this was primarily due to a loss of proliferation of cortical progenitor cells. The thin cortex, in the *Arx*$^{-/Y}$ *Emx1*^{Cre}, was primarily due to the animals specifically missing superficial layer neurons, whereas deeper layer neurons were predominately spared (Colasante et al. 2015). Most importantly, unlike the germline mutant mice, *Arx*$^{-/Y}$ *Emx1*^{Cre} mice do not die at a young age allowing for the complete behavioral characterization that we performed.

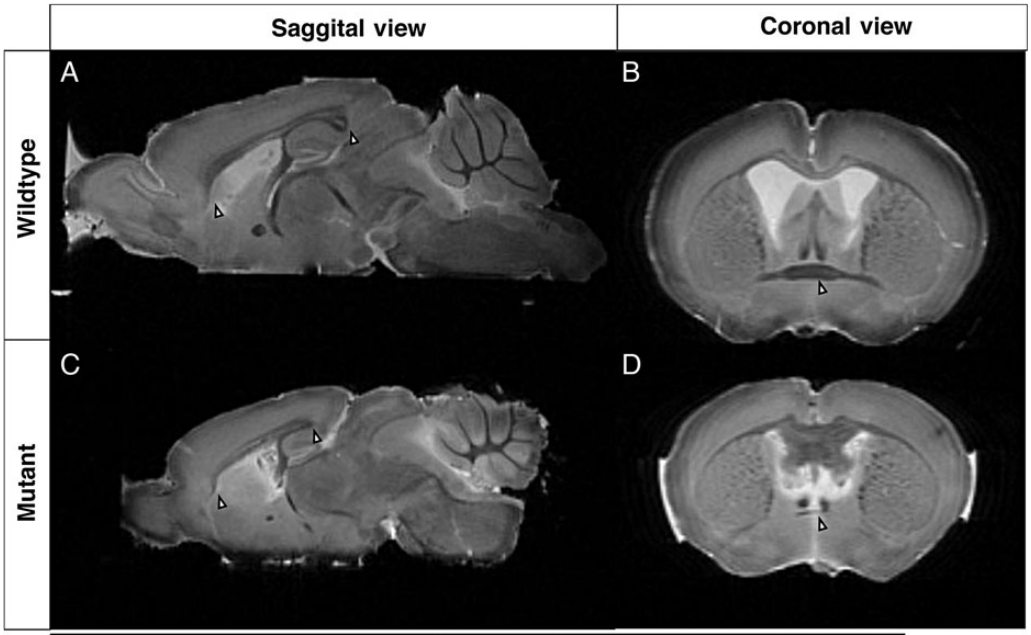

E

	WT	Mut	Percentage change	P-value
Cortex volume	122.77	86.88	-29.23	0.00616
Hippocampus volume	27.53	20.64	-25.05	0.07666
Amygdala volume	8.39	5.42	-35.40	0.00728
Thalamus volume	20.59	15.86	-22.96	0.02900
Basal ganglia volume	19.52	15.28	-21.71	0.12430
Corpus callosum volume	10.57	8.28	-21.69	0.04382

Figure 5. *Arx*$^{-/Y}$ *Emx1-Cre* mice have hypoplastic corpus callosums and anterior commissures. MRIs were made of 3 brains from mutant mice and 3 from their wild-type littermates. (*A*) A midsagittal section from an MRI of a wild-type brain (0.65 mm lateral to bregma). The white arrows mark the rostral and caudal ends of a normal corpus callosum. (*C*) A midsagittal section from an MRI of a mutant brain (0.65 mm lateral to bregma). The white arrows again mark the ends of the corpus callosum, showing that the corpus callosum is both shorter and thinner in the mutant mice. (*B*) A rostral coronal section from an MRI of a wild-type brain (0.14 mm posterior to bregma). The white arrow marks the middle of the anterior commissure. (*D*) A rostral coronal section from an MRI of a mutant brain (0.14 mm posterior to bregma). The white arrow marks the middle of the anterior commissure, showing that in the mutant it is much thinner. (*E*) Table of volumes (mm^3) of brain regions of wild-type and mutant mice from T_2-weighted MRI data and comparisons between the wild-type and mutant volumes for each region.

We hypothesize that the *Arx*$^{-/Y}$ *Emx1*^{Cre} mice survive because of a lack of seizures (Fig. 1*A*) and intact olfaction allowing for normal feeding behaviors when young. Consistent with a lack of seizures, *Arx*$^{-/Y}$ *Emx1*^{Cre} mice do not have a loss of interneurons in their cortices (Fig. 1*B*) and may have an increased level of inhibition due to the reduction in cortical size, but preserved numbers of interneurons. Therefore, we wanted to examine the behavioral phenotype of these mice to determine the impact on cortical functioning of isolated loss of upper layer neurons, without the complicating factors of interneuron loss and seizures as found in all other *Arx* mutant mice models.

Comparing the behavioral profiles of the *Arx*$^{-/Y}$ *Emx1*^{Cre} mice with the other *Arx* mutant mouse lines revealed a few interesting insight into the possible function of specific brain circuits and regions. The *Arx*$^{-/Y}$ *Emx1*^{Cre} animals had normal learning and memory in the Morris water maze and fear-conditioning paradigms (Fig. 2*A*–*E*) which contrast with all the viable knock-in mice (*Arx*$^{(GCG)7/Y}$, *Arx*$^{PI/Y}$ mice, and *Arx*$^{(GCG)10+7}$), which all had some degree of spatial learning or fear-conditioning deficit (Kitamura et al. 2009; Price et al. 2009).

In contrast to the differences between the *Arx*$^{-/Y}$ *Emx1*^{Cre} mice and the other *Arx* mutant mouse lines in learning and memory tasks, all the *Arx* mutant mouse lines had some disturbance in handling of stressful stimuli (anxiety behaviors). The *Arx*$^{-/Y}$ *Emx1*^{Cre} mice registered less anxiety-like behavior and were hyperactive (Fig. 3*A*,*B*); similar to the *Arx*$^{(GCG)10+7}$ mice (Price et al. 2009). The other *Arx* mutant mice (*Arx*$^{(GCG)7/Y}$ and *Arx*$^{PI/Y}$ mice) also exhibited abnormal anxiety-like behaviors, but were more anxious in the same tests (Kitamura et al. 2009).

Analysis of social deficits and stereotypies in the different *Arx* mutant mouse lines was also consistent with our *Arx*$^{-/Y}$ *Emx1*^{Cre} mice having social deficits in the social choice test (Fig. 4*A*), which matched the *Arx*$^{(GCG)10+7}$ line (Price et al. 2009). All together, the interpretation of the differences and similarities of these behaviors in multiple lines revealed that loss of interneurons, presence of seizures, and/or the interaction with cortical layer dysfunction is sufficient to generate a learning deficit. In contrast, only having abnormal layer 2–3 structure and the resultant absence of local and long-range projection pathways are sufficient for anxiety, social, and activity defects.

Cortical and subcortical structure and major projection pathways were further evaluated in the *Arx*$^{-/Y}$ *Emx1*^{Cre} mice. The *Arx*$^{-/Y}$ *Emx1*^{Cre} mice were found to have decreased cerebral cortical and amygdala volumes by MRI as well as severely diminished interhemispheric tracts (callosum and anterior commissure). The cortical volume deficits are presumably due to the previously described substantial reduction in the layer 2–3 neuronal population (Colasante et al. 2015). The layer 2–3 changes are consistent with the loss of the local and

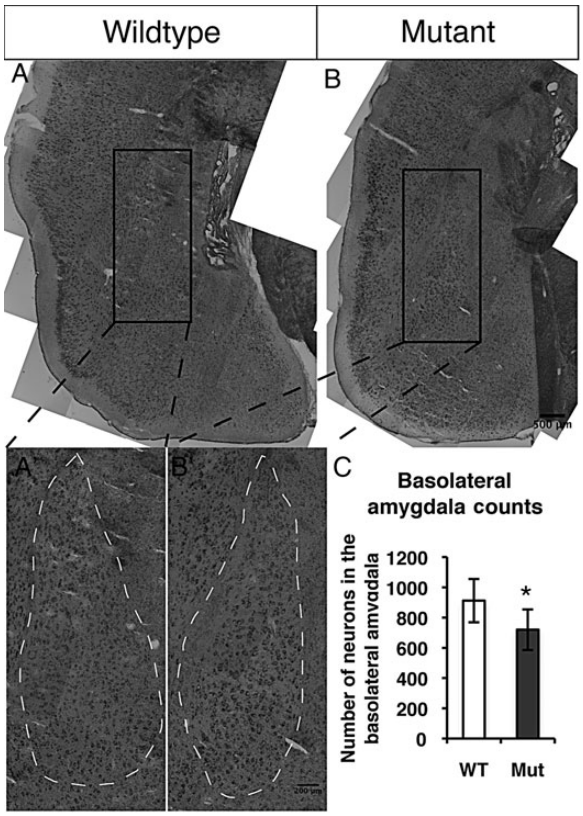

Figure 6. *Arx*$^{-/Y}$ *Emx1-Cre* mice have a loss of neurons in the basolateral amygdala. (*A* and *B*) Coronal brain sections of adult mutant mice and their wild-type littermates were stained with Nissl, which labels all neurons. (*A′* and *B′*) Enlarged sections showing the basolateral amygdala region (dotted white outline) which was counted. (*C*) Quantification of the number of neurons counted in the basolateral amygdala of the *Arx*$^{-/Y}$ *Emx1-Cre* mice and their wild-type littermates, showing that the mutant mice have fewer neurons in the basolateral amygdala when compared with wild-type littermates (WT = 1118 ± 124 and Mut = 891 ± 152, $n = 3$ for each; $P = 0.01952$). Error bars are SE.

interhemispheric projection pathways as layer 2–3 neurons are the primary cortical layer that sends axons into the callosum and anterior commissure. The finding of ACC was reported in *Arx*$^{-/y}$ mice, but not in the *Arx*$^{(GCG)10+7}$, *Arx*$^{(GCG)7/Y}$, *Arx*$^{PL/Y}$, or *Arx*$^{PR/Y}$ mice (Kitamura et al. 2002, 2009; Price et al. 2009). We postulate that each mutation differentially alters Arx binding resulting in separate effects on developing cortical and subcortical progenitors with an end result of seizures but an intact CC in the knock-in and interneuron deletion models, no seizures but ACC in the *Arx*$^{-/Y}$ *Emx1*^{Cre} line, and both seizures and ACC in the complete knock-out. The differential effect on Arx binding, therefore, likely explains the genotype–phenotype correlation observed in humans. This finding of ACC in some of the mouse lines but not others recapitulates that the human condition as ACC has also been documented in some *ARX* patients with XLAG or Proud syndrome and heterozygous females but not all patients (Proud et al. 1992; Bonneau et al. 2002; Marsh et al. 2009). Interestingly, there is no clear relationship between the presence of a normal corpus callosum and the extent of cognitive disabilities.

In addition to adding insights into the possible structure–function relationships that the *Arx*$^{-/Y}$ *Emx1*^{Cre} mice provide, an interpretation of the role of seizures in generating behaviors can be hypothesized. Indeed, neurologists have questioned the ultimate role of seizures in generating the cognitive deficits in their patients (Shinnar and Hauser 2002; Hamiwka and Wirrell 2009; Hermann et al. 2009). The absence of seizures in the *Arx*$^{-/Y}$ *Emx1*^{Cre} mice demonstrated that the mice still have altered anxiety, hyperactivity, and social deficits a core set of symptoms reminiscent of patients with mild *ARX* phenotypes. As patients do not have loss of *ARX* from a subset of cells, the human condition is clearly more complex; however, our studies imply that at least some behaviors (i.e., alterations in anxiety, hyperactivity, and social deficits) are unrelated to the epilepsy. Indeed, some of the "mild" *ARX* patients reported are without seizures but with cognitive and social deficits (Turner et al. 2002).

The recordings that demonstrated a lack of seizures also revealed differences in the frequency composition of the EEG between the *Arx*$^{-/Y}$ *Emx1*^{Cre} and wild-type mice. The slow background and an increase in Delta activity in the mutant mice are reminiscent of the EEG findings in many children with a diffuse encephalopathy, including children with *ARX* mutations. Though nonspecific, a slow EEG background suggests diffuse brain dysfunction as might be expected in a cortical layer defect (Pedley 1980). Interestingly, the composition of the EEG in the *Arx*$^{-/Y}$ *Emx1*^{Cre} and *Arx*$^{-/Y}$ *Dlx5/6*^{Cre} is different, with the interneuron-specific mouse (*Arx*$^{-/Y}$ *Dlx5/6*^{Cre}) gaining faster frequency activity and the excitatory neuron-specific mouse (*Arx*$^{-/Y}$ *Emx1*^{Cre}) gaining slower activity (Marsh et al. 2009). This difference supports the notion that interneurons and subcortical structures are necessary for the generation of Theta and Gamma oscillations, and local cortical networks are not (Bragin et al. 1995; Whittington et al. 2011).

Overall, the *Arx*$^{-/Y}$ *Emx1*^{Cre} mouse line with the other conditional and mutant *Arx* mice that have been generated offers an opportunity to dissect apart a complex circuit to look for local circuit or regional connections that are necessary or sufficient for the generation of complex behaviors. We acknowledge at the onset that this is a difficult endeavor as any one change in a developing system alters the others, and that both cognitive and social behaviors are complex tasks that involve the function of networks, not just cortical regions and layers. With those caveats in mind, our findings suggest an important role for superficial cortical regions and the amygdala, in the generation of a hyperactive, anxiolytic, anti-social phenotype.

Supplementary Material

Supplementary material can be found at: http://www.cercor.oxfordjournals.org/.

Funding

This work was supported by the National Institutes of Health (NS46616 and HD26979 to J.A.G., NS065975 and NS082761 to E.D.M. and the Neurodevelopmental Disabilities Training Grant T32NS007413).

Notes

We thank Dr Ted Abel, Dr Ted Brodkin, Dr Tracy Bale, and Dr Irwin Lucki for their consultations about behavioral experimental methods and analysis. In addition, we thank Dr Kunio Kitamura for the anti-Arx antibody and George Clement for his assistance with animal husbandry, genotyping, and behavioral assays. We also thank Guy LeBas and

Christina Bradley for their assistance with behavioral assays, Elliot Bourgeois for writing the MATLAB code for home cage movement detection, and Camillo Bermudez and Irfan Shehzad for assistance with the EEG quantification. Finally, we thank all the members of the Golden lab past and present and Drs Michael Granto, Matthew Dalva, Erika Holzbauer, and Paul Janmey for helpful discussions. *Conflict of Interest*: None declared.

References

Albarran-Zeckler RG, Brantley AF, Smith RG. 2012. Growth hormone secretagogue receptor (GHS-R1a) knockout mice exhibit improved spatial memory and deficits in contextual memory. Behav Brain Res. 232:13–19.

Angelo M, Plattner F, Irvine EE, Giese KP. 2003. Improved reversal learning and altered fear conditioning in transgenic mice with regionally restricted p25 expression. Eur J Neurosci. 18:423–431.

Azim E, Jabaudon D, Fame RM, Macklis JD. 2009. SOX6 controls dorsal progenitor identity and interneuron diversity during neocortical development. Nat Neurosci. 12:1238–1247.

Bale TL, Contarino A, Smith GW, Chan R, Gold LH, Sawchenko PE, Koob GF, Vale WW, Lee KF. 2000. Mice deficient for corticotropin-releasing hormone receptor-2 display anxiety-like behaviour and are hypersensitive to stress. Nat Genet. 24:410–414.

Bonneau D, Kaplan J, Girard G, Dufier JL. 1992. Autosomal inheritance of "senile" retinitis pigmentosa. A report of a family with consanguinity. Clin Genet. 42:199–200.

Bonneau D, Toutain A, Laquerriere A, Marret S, Saugier-Veber P, Barthez MA, Radi S, Biran-Mucignat V, Rodriguez D, Gelot A. 2002. X-linked lissencephaly with absent corpus callosum and ambiguous genitalia (XLAG): clinical, magnetic resonance imaging, and neuropathological findings. Ann Neurol. 51:340–349.

Bourin M, Hascoet M. 2003. The mouse light/dark box test. Eur J Pharmacol. 463:55–65.

Bragin A, Jando G, Nadasdy Z, Hetke J, Wise K, Buzsaki G. 1995. Gamma (40–100 Hz) oscillation in the hippocampus of the behaving rat. J Neurosci. 15:47–60.

Buschert J, Hohoff C, Touma C, Palme R, Rothermundt M, Arolt V, Zhang W, Ambree O. 2013. S100B overexpression increases behavioral and neural plasticity in response to the social environment during adolescence. J Psychiatr Res. 47(11):1791–1799.

Chioca LR, Antunes VD, Ferro MM, Losso EM, Andreatini R. 2013. Anosmia does not impair the anxiolytic-like effect of lavender essential oil inhalation in mice. Life Sci. 92:971–975.

Colasante G, Simonet JC, Calogero R, Crispi S, Sessa A, Cho G, Golden JA, Broccoli V. 2015. ARX regulates cortical intermediate progenitor cell expansion and upper layer neuron formation through repression of Cdkn1c. Cereb Cortex.25:322–335.

Cole JT, Mitala CM, Kundu S, Verma A, Elkind JA, Nissim I, Cohen AS. 2010. Dietary branched chain amino acids ameliorate injury-induced cognitive impairment. Proc Natl Acad Sci USA. 107:366–371.

Crawley JN. 2007. Mouse behavioral assays relevant to the symptoms of autism. Brain Pathol. 17:448–459.

d'Isa R, Clapcote SJ, Voikar V, Wolfer DP, Giese KP, Brambilla R, Fasano S. 2011. Mice lacking Ras-GRF1 show contextual fear conditioning but not spatial memory impairments: convergent evidence from two independently generated mouse mutant lines. Front Behav Neurosci. 5:78.

Deacon RM. 2006. Digging and marble burying in mice: simple methods for in vivo identification of biological impacts. Nat Protoc. 1:122–124.

Erlander MG, Tillakaratne NJ, Feldblum S, Patel N, Tobin AJ. 1991. Two genes encode distinct glutamate decarboxylases. Neuron. 7:91–100.

Fairless AH, Dow HC, Toledo MM, Malkus KA, Edelmann M, Li H, Talbot K, Arnold SE, Abel T, Brodkin ES. 2008. Low sociability is associated with reduced size of the corpus callosum in the BALB/cJ inbred mouse strain. Brain Res. 1230:211–217.

Fowler SC, Zarcone TJ, Vorontsova E, Chen R. 2002. Motor and associative deficits in D2 dopamine receptor knockout mice. Int J Dev Neurosci. 20:309–321.

Friocourt G, Kanatani S, Tabata H, Yozu M, Takahashi T, Antypa M, Raguenes O, Chelly J, Ferec C, Nakajima K et al. 2008. Cell-autonomous roles of ARX in cell proliferation and neuronal migration during corticogenesis. J Neurosci. 28:5794–5805.

Friocourt G, Poirier K, Rakic S, Parnavelas JG, Chelly J. 2006. The role of ARX in cortical development. Eur J Neurosci. 23:869–876.

Fulp CT, Cho G, Marsh ED, Nasrallah IM, Labosky PA, Golden JA. 2008. Identification of Arx transcriptional targets in the developing basal forebrain. Hum Mol Genet. 17:3740–3760.

Gecz J, Cloosterman D, Partington M. 2006. ARX: a gene for all seasons. Curr Opin Genet Dev. 16:308–316.

Golub MS, Germann SL. 2001. Long-term consequences of developmental exposure to aluminum in a suboptimal diet for growth and behavior of Swiss Webster mice. Neurotoxicol Teratol. 23:365–372.

Grillon C, Southwick SM, Charney DS. 1996. The psychobiological basis of posttraumatic stress disorder. Mol Psychiatr. 1:278–297.

Hamiwka LD, Wirrell EC. 2009. Comorbidities in pediatric epilepsy: beyond "just" treating the seizures. J Child Neurol. 24:734–742.

Han Q, Feng J, Qu Y, Ding Y, Wang M, So KF, Wu W, Zhou L. 2013. Spinal cord maturation and locomotion in mice with an isolated cortex. Neuroscience. 253:235–244.

Harris L, Dixon C, Cato K, Heng YH, Kurniawan ND, Ullmann JF, Janke AL, Gronostajski RM, Richards LJ, Burne TH et al. 2013. Heterozygosity for nuclear factor one x affects hippocampal-dependent behaviour in mice. PLoS ONE. 8:e65478.

Hermann BP, Lin JJ, Jones JE, Seidenberg M. 2009. The emerging architecture of neuropsychological impairment in epilepsy. Neurol Clin. 27:881–907.

Heyser CJ, Vishnevetsky D, Berten S. 2013. The effect of cocaine on rotarod performance in male C57BL/6J mice. Physiol Behav. 118:208–211.

Jin XL, Guo H, Mao C, Atkins N, Wang H, Avasthi PP, Tu YT, Li Y. 2000. Emx1-specific expression of foreign genes using "knock-in" approach. Biochem Biophys Res Commun. 270:978–982.

Kitamura K, Itou Y, Yanazawa M, Ohsawa M, Suzuki-Migishima R, Umeki Y, Hohjoh H, Yanagawa Y, Shinba T, Itoh M et al. 2009. Three human ARX mutations cause the lissencephaly-like and mental retardation with epilepsy-like pleiotropic phenotypes in mice. Hum Mol Genet. 18:3708–3724.

Kitamura K, Yanazawa M, Sugiyama N, Miura H, Iizuka-Kogo A, Kusaka M, Omichi K, Suzuki R, Kato-Fukui Y, Kamiirisa K et al. 2002. Mutation of ARX causes abnormal development of forebrain and testes in mice and X-linked lissencephaly with abnormal genitalia in humans. Nat Genet. 32:359–369.

Krass M, Runkorg K, Wegener G, Volke V. 2010. Nitric oxide is involved in the regulation of marble-burying behavior. Neurosci Lett. 480:55–58.

Lafaucheur L, Missohou A, Ecolan P, Monin G, Bonneau M. 1992. Performance, plasma hormones, histochemical and biochemical muscle traits, and meat quality of pigs administered exogenous somatotropin between 30 or 60 kilograms and 100 kilograms body weight. J Anim Sci. 70:3401–3411.

Lin CH, Jao WC, Yeh YH, Lin WC, Yang MC. 2009. Hemocompatibility and cytocompatibility of styrenesulfonate-grafted PDMS-polyurethane-HEMA hydrogel. Colloids Surf B Biointerfaces. 70:132–141.

Lodato S, Rouaux C, Quast KB, Jantrachotechatchawan C, Studer M, Hensch TK, Arlotta P. 2011. Excitatory projection neuron subtypes control the distribution of local inhibitory interneurons in the cerebral cortex. Neuron. 69:763–779.

Marsh E, Fulp C, Gomez E, Nasrallah I, Minarcik J, Sudi J, Christian SL, Mancini G, Labosky P, Dobyns W et al. 2009. Targeted loss of Arx results in a developmental epilepsy mouse model and recapitulates the human phenotype in heterozygous females. Brain. 132:1563–1576.

Medina L, Legaz I, Gonzalez G, De Castro F, Rubenstein JL, Puelles L. 2004. Expression of Dbx1, Neurogenin 2, Semaphorin 5A, Cadherin 8, and Emx1 distinguish ventral and lateral pallial histogenetic divisions in the developing mouse claustroamygdaloid complex. J Comp Neurol. 474:504–523.

Miwa JM, Walz A. 2012. Enhancement in motor learning through genetic manipulation of the Lynx1 gene. PLoS ONE. 7:e43302.
Moy SS, Nadler JJ, Perez A, Barbaro RP, Johns JM, Magnuson TR, Piven J, Crawley JN. 2004. Sociability and preference for social novelty in five inbred strains: an approach to assess autistic-like behavior in mice. Genes Brain Behav. 3:287–302.
Munn E, Bunning M, Prada S, Bohlen M, Crabbe JC, Wahlsten D. 2011. Reversed light-dark cycle and cage enrichment effects on ethanol-induced deficits in motor coordination assessed in inbred mouse strains with a compact battery of refined tests. Behav Brain Res. 224:259–271.
Nadler JJ, Moy SS, Dold G, Trang D, Simmons N, Perez A, Young NB, Barbaro RP, Piven J, Magnuson TR et al. 2004. Automated apparatus for quantitation of social approach behaviors in mice. Genes Brain Behav. 3:303–314.
Pedley TA. 1980. Interictal epileptiform discharges: discriminating characteristics and clinical correlations. Am J Electroencephalogr Technol. 20:101–119.
Phillips RG, LeDoux JE. 1992. Differential contribution of amygdala and hippocampus to cued and contextual fear conditioning. Behav Neurosci. 106:274–285.
Poirier K, Van Esch H, Friocourt G, Saillour Y, Bahi N, Backer S, Souil E, Castelnau-Ptakhine L, Beldjord C, Francis F et al. 2004. Neuroanatomical distribution of ARX in brain and its localisation in GABAergic neurons. Brain Res Mol Brain Res. 122:35–46.
Price MG, Yoo JW, Burgess DL, Deng F, Hrachovy RA, Frost JD Jr, Noebels JL. 2009. A triplet repeat expansion genetic mouse model of infantile spasms syndrome, Arx(GCG)10+7, with interneuronopathy, spasms in infancy, persistent seizures, and adult cognitive and behavioral impairment. J Neurosci. 29:8752–8763.
Proud VK, Levine C, Carpenter NJ. 1992. New X-linked syndrome with seizures, acquired micrencephaly, and agenesis of the corpus callosum. Am J Med Genet. 43:458–466.
Puelles L, Kuwana E, Puelles E, Bulfone A, Shimamura K, Keleher J, Smiga S, Rubenstein JL. 2000. Pallial and subpallial derivatives in the embryonic chick and mouse telencephalon, traced by the expression of the genes Dlx-2, Emx-1, Nkx-2.1, Pax-6, and Tbr-1. J Comp Neurol. 424:409–438.
Remedios R, Huilgol D, Saha B, Hari P, Bhatnagar L, Kowalczyk T, Hevner RF, Suda Y, Aizawa S, Ohshima T et al. 2007. A stream of cells migrating from the caudal telencephalon reveals a link between the amygdala and neocortex. Nat Neurosci. 10:1141–1150.
Rudy B, Fishell G, Lee S, Hjerling-Leffler J. 2011. Three groups of interneurons account for nearly 100% of neocortical GABAergic neurons. Dev Neurobiol. 71:45–61.
Sankoorikal GM, Kaercher KA, Boon CJ, Lee JK, Brodkin ES. 2006. A mouse model system for genetic analysis of sociability: C57BL/6J versus BALB/cJ inbred mouse strains. Biol Psychiatry. 59:415–423.
Schienle A, Ebner F, Schafer A. 2011. Localized gray matter volume abnormalities in generalized anxiety disorder. Eur Arch Psychiatry Clin Neurosci. 261:303–307.
Sessa A, Mao CA, Colasante G, Nini A, Klein WH, Broccoli V. 2010. Tbr2-positive intermediate (basal) neuronal progenitors safeguard cerebral cortex expansion by controlling amplification of pallial glutamatergic neurons and attraction of subpallial GABAergic interneurons. Genes Dev. 24:1816–1826.
Shinnar S, Hauser WA. 2002. Do occasional brief seizures cause detectable clinical consequences? Prog Brain Res. 135:221–235.
Shoubridge C, Fullston T, Gecz J. 2010. ARX spectrum disorders: making inroads into the molecular pathology. Hum Mutat. 31:889–900.
Silverman JL, Yang M, Lord C, Crawley JN. 2010. Behavioural phenotyping assays for mouse models of autism. Nat Rev Neurosci. 11:490–502.
Suri M. 2005. The phenotypic spectrum of ARX mutations. Dev Med Child Neurol. 47:133–137.
Thomas A, Burant A, Bui N, Graham D, Yuva-Paylor LA, Paylor R. 2009. Marble burying reflects a repetitive and perseverative behavior more than novelty-induced anxiety. Psychopharmacology (Berl). 204:361–373.
Tottenham N, Hare TA, Quinn BT, McCarry TW, Nurse M, Gilhooly T, Millner A, Galvan A, Davidson MC, Eigsti IM et al. 2010. Prolonged institutional rearing is associated with atypically large amygdala volume and difficulties in emotion regulation. Dev Sci. 13:46–61.
Turner G, Partington M, Kerr B, Mangelsdorf M, Gecz J. 2002. Variable expression of mental retardation, autism, seizures, and dystonic hand movements in two families with an identical ARX gene mutation. Am J Med Genet. 112:405–411.
Vorhees CV, Williams MT. 2006. Morris water maze: procedures for assessing spatial and related forms of learning and memory. Nat Protoc. 1:848–858.
Whittington MA, Cunningham MO, LeBeau FE, Racca C, Traub RD. 2011. Multiple origins of the cortical gamma rhythm. Dev Neurobiol. 71:92–106.
Wood MA, Kaplan MP, Park A, Blanchard EJ, Oliveira AM, Lombardi TL, Abel T. 2005. Transgenic mice expressing a truncated form of CREB-binding protein (CBP) exhibit deficits in hippocampal synaptic plasticity and memory storage. Learn Mem. 12:111–119.
Xu X, Roby KD, Callaway EM. 2010. Immunochemical characterization of inhibitory mouse cortical neurons: three chemically distinct classes of inhibitory cells. J Comp Neurol. 518:389–404.
Yang M, Crawley JN. 2009. Simple behavioral assessment of mouse olfaction. Curr Protoc Neurosci. Chapter 8: Unit 8. 24. doi:10.1002/0471142301.ns0824s48